

Thermoreflectance and temperature dependence of the $L_{2,3}$ soft-x-ray threshold in Si

D. E. Aspnes[†]

*Bell Laboratories, Murray Hill, New Jersey 07974**
and Max-Planck-Institut für Festkörperforschung, 7000 Stuttgart 80, Federal Republic of Germany

R. S. Bauer, R. Z. Bachrach, and J. C. McMennamin

Xerox Palo Alto Research Center, Palo Alto, California 94304

(Received 5 May 1977)

We report thermoreflectance and temperature-dependent reflectance data for the 100-eV $L_{2,3}$ soft-x-ray threshold of Si. The thermoreflectance data show that the threshold energy shift with temperature accounts for nearly all features of the observed line shape. Only minor contributions arise from changes in broadening parameters. The reflectance data show that the total shift of the $j = 3/2$ threshold to lower energy as the temperature is increased from 150 to 600 K is surprisingly large, 250 ± 50 meV. The major contribution to this shift appears to be the change of the electrostatic potential at the $2p$ core sites resulting from the reduction of bond charge with increasing temperature. This large temperature dependence is incompatible with the lattice-mode model, which could explain the data only if a single core hole could destroy $2e$ of bond charge.

I. INTRODUCTION

The temperature dependences of critical-point energies in the joint densities of states of sp^3 valence-conduction-band transitions of tetrahedrally bonded semiconductors are now fairly well understood. These have been interpreted either as a perturbation of one-electron energy levels by the temperature-dependent population of phonons,¹⁻⁵ or as a softening of lattice modes caused by the reduction of bond charge resulting from the creation of a single electron-hole pair.^{6,7} The different approaches give the same results for valence-conduction-band absorption threshold, where the relative temperature shifts arise from electron-phonon interactions alone.²

By contrast, the temperature dependences of transitions from core levels to the sp^3 conduction bands are more complicated. Measurements of transitions from the 19-eV deep Ga- $3d$ core levels to the X_6^C conduction-band minima in GaP show clearly that volume effects play a significant role.⁸ By calculating the magnitude of the volume and phonon effects on the one-electron energy levels, it was shown that the GaP results could be explained entirely on the basis of temperature-induced shifts of the one-electron energy levels of the conduction band. No temperature shift of the core levels appeared to occur. This result suggests that the temperature-induced energy shifts of core levels in general may be small relative to those of the more extended outer bonding-antibonding electron levels.

To investigate the generality of this conclusion, the effectiveness of modulation techniques in the soft-x-ray region, and the applicability of the one-

electron and lattice-mode theories of the temperature dependence of absorption edges for core-level transitions, we have obtained new high-precision reflectance and thermoreflectance (TR) spectra on the deeper more-localized Si $2p_{3/2}$ and $2p_{1/2}$ core levels responsible for the 100-eV $L_{2,3}$ soft-x-ray threshold of Si, and have measured their temperature shifts from 150 to 600 K. These transitions give rise to sharp edge structure in optical spectra which has been studied by reflectance^{9,10} and transmittance¹¹ in crystalline material, and by transmittance in polycrystalline and amorphous films.^{12,13} By contrast to the GaP results, the energies of the Si- $2p$ core levels appear to be strongly affected by temperature. This strong temperature dependence cannot be explained within the lattice-mode theory.

II. EXPERIMENTAL

All measurements were performed on the 4° beam line at the Stanford Synchrotron Radiation Project, using synchrotron radiation from the electron storage ring of SPEAR. The effective resolution for these measurements in the 100-eV spectral region was 0.15 eV. Samples consisted of 0.6- Ω cm single-crystal n -type Si ribbons, having approximate dimensions of $0.25 \times 5 \times 25$ mm³. The Syton-polished reflecting surfaces were (111) planes.

All optical measurements were made at an angle of incidence of $85.0^\circ \pm 0.3^\circ$, as determined from the detector positions in normal and straight-through operation. This value is near the angle (80°) that maximizes the signal-to-noise ratio, as calculated¹⁴ using the measured¹⁰ optical constants

of Si near 100 eV. A two-stage chevron-channel-plate-detector system was used in the single-beam mode to measure the intensity of the reflected light. Approximate absolute reflectance calibration ($\pm 20\%$) was obtained by measuring the intensity in straight-through operation, and by scaling all data points inversely with respect to the storage ring current.

The signal-to-noise ratio was further improved by using a boxcar-gated averager before the phase-sensitive detector. By this means, only the information-containing detector output, centered about the 0.3-nsec photon pulse, was transmitted to the rest of the data-acquisition system.¹⁵ This novel method of matching the time-averaging characteristic of the phase-sensitive detector to the output of a synchrotron radiation source is discussed in detail elsewhere.¹⁶ Signal-to-noise limits obtained by this technique were about 10^{-3} and 10^{-4} at 0.5 Hz and 100 Hz, respectively, for averaging times of 30 sec.

Low-temperature and room-temperature reflectance measurements were made with the samples nominally attached to a liquid-nitrogen cold finger, which was covered by a thin mica sheet to provide electrical isolation. High-temperature reflectance and thermoreflectance spectra were obtained by passing current directly through the samples by means of Ohmic contacts at the ends. For the latter measurements, a 0.5-Hz 12-W square-wave heating cycle was used. This resulted in a sample temperature variation of about 70 °C centered about a mean value of 330 °C, as inferred from on-line resistance measurements compared to later direct calibration of the resistance versus temperature behavior of this material. The relatively large-amplitude thermal cycling invariably caused the Si ribbons to separate from the cold-finger mounting. Thus, the high-temperature data (and some of the room-temperature and low-temperature data as well) were for free-standing Si ribbons supported and cooled through the end contacts. Because sample temperatures were not measured directly, and because data from both cold-finger and free-standing configurations were used in analysis, we estimate the uncertainty in all temperatures as ± 50 °C. This is not overly serious, because thermal effects saturate at low temperature and the total range measured was about 450 °C.

III. RESULTS

The experimental results are summarized in Figs. 1–3. Figure 1 shows representative reflectance data from a free-standing Si ribbon for three different temperatures. No smoothing was required for these spectra. These data have been

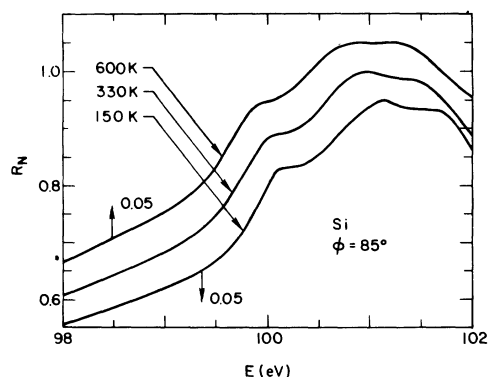


FIG. 1. Normalized reflectance spectra of crystalline Si at the $L_{2,3}$ soft-x-ray threshold. The spectra have been offset as indicated for clarity.

normalized to a peak value of unity, and the 600- and 150-K curves have been offset by 0.05 as indicated for clarity. The numerically calculated first derivatives of these normalized spectra are shown in Fig. 2. In Fig. 3, the top curve is the temperature-induced change ΔR of the unnormalized reflectance spectrum that was obtained using the modulation conditions described in Sec. II. The numerically calculated first energy derivative of the unnormalized reflectance, measured concurrently with ΔR , is shown in the middle of Fig. 3. The bottom spectrum of Fig. 3 shows the properly normalized measured thermoreflectance spectrum, $\Delta R/R$.

The spectra of Figs. 1–3 show clearly the reflectance structures due to the onset of transitions between the $j = \frac{1}{2}$ and $j = \frac{3}{2}$ $2p$ core levels and the bottom of the sp^3 conduction band. Using the dielectric function¹⁰ of Si in this spectral region,

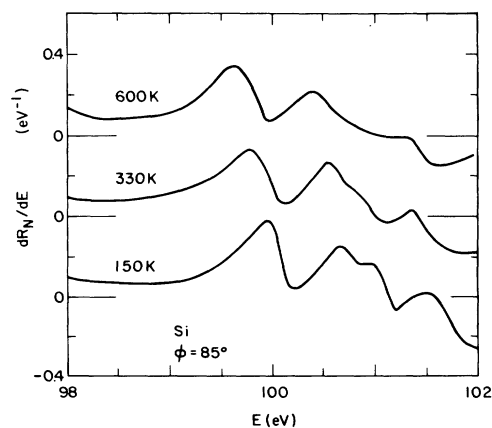


FIG. 2. First-derivative spectra of Si at the $L_{2,3}$ soft-x-ray threshold calculated numerically from the normalized spectra of Fig. 1.

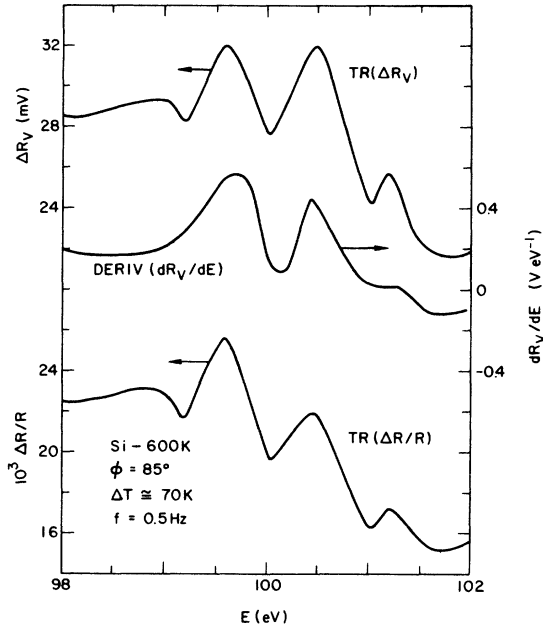


FIG. 3. Top: unnormalized temperature-induced change ΔR in the unnormalized reflectance obtained under modulation conditions described in the text. Middle: numerically calculated first energy derivative of the unnormalized reflectance data obtained concurrently with ΔR . Bottom: standard properly normalized thermoreflectance spectrum.

we calculate that structure in R arises from corresponding structure in $(\epsilon_1 - 1)$ and ϵ_2 in approximately a 2 : 3 ratio. Thus although the absorption line shape dominates in determining the reflectance line shape there is nevertheless a substantial admixture of its Kramers-Kronig transform. For this reason, we believe that the threshold and spin-orbit splitting energies^{12,13} of 99.84 ± 0.06 and 0.61 ± 0.02 eV, respectively, determined from the point of maximum slope of the optical density spectrum for thin polycrystalline films, are more reliable than values that could be inferred from the corresponding line shapes of Fig. 2.

We can, however, obtain accurate temperature-shift data from the spectra of Fig. 2. Because the Varshni β parameter is so large (636 ± 50 K)¹⁷ for Si, and because its thermal expansion properties¹⁸ are so nonlinear, it is more useful to discuss the temperature dependence as a difference between the 150- and 600-K values. We find that the apparent shift of the threshold of the Si $2p_{3/2} \rightarrow \Delta_1$ transition between 150 and 600 K is -250 ± 50 meV, as indicated in Table I. The same value is obtained from all spectral features associated with the $j = \frac{3}{2}$ threshold. This is expected since the line shape is determined by shift and not broadening effects (see below). By comparison, the shift in the fundamental indirect gap over the same tem-

TABLE I. Summary of temperature-shift data and calculated contributions for the $L_{2,3}$ soft-x-ray threshold of Si, expressed as a difference of threshold energies at 150 and 600 K.

Quantity	Si-2p	$\Delta_1^C(X_1^C)$	Net contribution
Debye-Waller	...	-48 meV ^a	-48 meV
Self-energy	...	(small)	~0
Hydrostatic	+6 meV	-30	-36
V_{000}	...	+9	+9
Bond charge	+170 (?)	...	-170 (?)
Experimental	-250 ± 50 meV

^aCamassel and Auvergne, Ref. 4.

perature range is about half as large, -124 meV.^{17,19,20}

The unnormalized ΔR spectrum at the top of Fig. 3 shows immediately by its similarity to the unnormalized dR/dE spectrum in the middle that temperature-modulation results almost entirely from the shift of the thresholds to lower energy with increasing temperature, rather than an increase in the broadening parameter. The thermoreflectance spectrum nevertheless shows some surprising features that are not immediately obvious from the derivative data of Fig. 2. Both the $j = \frac{1}{2}$ core-level structure at 100.5 eV and the feature near 101.1 eV are significantly larger in the TR data than are their counterparts in the derivative spectrum, indicating that these thresholds vary more rapidly with temperature than the $j = \frac{3}{2}$ thresholds. The more rapid temperature shift of the $j = \frac{1}{2}$ core level is surprising, and we have no explanation for it at present. Similar behavior has been noted in thermoreflectance measurements at the spin-orbit-split $E_1 + \Delta_1$ transition in a number of zinc-blende semiconductors.²¹

The rapid temperature dependence of the small structure near 101.1 eV in Fig. 3 can be explained qualitatively by assigning the initial state to $j = \frac{1}{2}$ and the final state to the more strongly temperature-dependent second conduction-band minimum at L_1^C .¹² The initial-state assignment is further supported by the appearance of a $j = \frac{3}{2}$ component in the 150-K spectrum of Fig. 2, where the more rapid final-state temperature dependence enables it to move out from behind the larger $2p_{3/2} - X_1^C$ structure. We note, however, that assignments of final-state wave functions to localized regions of the Brillouin zone are not consistent with the observed binding energy of hundreds of meV^{11,16} of the core-level exciton at the $j = \frac{3}{2} - \Delta_1^C$ threshold. This interaction must clearly mix conduction-band wave functions over a relatively large region of the Brillouin zone (although different final states will contain different proportions of band-struct-

ture states). For this reason, the apparent 0.9-eV separation of the Δ_1^C and L_1^C features is probably not representative of the actual $L_1^C - \Delta_1^C$ separation in this material. This value agrees closely with the predictions of nonlocal pseudopotential calculations.²² However, since experiments²³ indicate a somewhat smaller value the issue has not been completely resolved.

IV. MODEL CALCULATION

Despite the complications of making symmetry assignments, it is useful to estimate the various contributions to the total temperature shift from band theory. The final-state electron-hole excitation should show at least some correlation to the unperturbed levels, for which a calculation is possible. We shall work in the framework wherein electrons are perturbed by phonons and the sp^3 conduction-band shifts are calculated with respect to the V_{000} pseudopotential reference. We shall comment about the alternate approach below.

For X_6^C , Camassel and Auvergne⁵ calculated a Debye-Waller contribution of -1.07×10^{-4} eV K⁻¹ from 200 to 300 K using the nonlocal pseudopotential coefficients of Chelikowsky and Cohen²²; extrapolation to the 150–600-K range yields a total shift of -48 meV for X_6^C . The self-energy terms^{3,4} are generally taken to be small, and indeed this appears to be the case in III-V compounds where TO-phonon scattering predominates.⁴ The result is less obvious for Si, where the effect of an indirect-gap $\Gamma_8^V - \Delta_6^C$ electron-hole excitation on the TA lattice modes has been shown to account well for the observed temperature dependence of the indirect gap over a wide range of temperature.⁷ Nevertheless, the total Debye-Waller contribution of the indirect gap was observed to agree with experiment over the 200–300-K range, where TA anharmonicity effects are not yet significant. Thus, it appears that self-energy terms are small as well in Si.

The hydrostatic term describing the effect of lattice expansion of the Fermi level of the valence-charge distribution is calculated by the method of Cardona²⁴ from pseudopotential form factors.²⁵ Since the total linear expansion $\Delta a_0/a_0$ ($a_0 = 10.263a_B$, where a_0 is the lattice constant) is about 1.25×10^{-3} from 150 to 600 K,¹⁸ the hydrostatic term contributes a total shift of -30 meV. Calculating this term in a simple Fermi gas model yields -31 meV. The V_{000} pseudopotential term⁸ $-\frac{3}{2}\epsilon_0^{-2/3}a_0(dE_F/da_0)$ has a value of $+9$ meV and thus partially cancels the hydrostatic contribution.

Summing the above contributions yields a net theoretical sp^3 conduction-band shift of -69 meV, much less than the observed shift of -250 ± 50 meV

over the 150–600-K temperature interval. Thus either the “binding energy” of the electron- $L_{2,3}$ -core-hole pair must have an intrinsically large temperature dependence, or else the energy of the core electrons must be shifting relative to the valence-band edge in response to the temperature-induced redistribution of valence charge. We consider the latter possibility explicitly, because the former is not expected to be strongly temperature dependent.

The temperature dependence of the electrostatic potential of the valence charge at the Ga nucleus in GaP was estimated theoretically in model calculations and was found to be large in principle. However, calculated values were found to be quite sensitive to assumptions about the detailed spatial variation of the unperturbed valence and core charge and the temperature-induced redistribution of this charge.⁸ Therefore, the intuitively reasonable experimental result of little or no apparent electrostatic shift of the Ga-3d core levels in GaP was accepted without further attempted interpretation.

In view of the new data for Si, however, it is worthwhile to estimate for this material the temperature-induced electrostatic shift at the core sites. This can be approximated in the Phillips bond-charge model²⁶ as arising from charges $-2e/\epsilon_0$ and $+4e/\epsilon_0$ at the bond sites and atomic core locations, respectively, where ϵ_0 is the static dielectric constant ($\epsilon_0 = 11.7$ for Si). We find²⁶

$$V = -20.6e/\epsilon_0 a_0, \quad (1a)$$

$$V(0) = -4.7 \text{ eV}, \quad (1b)$$

where the prefactor includes the Madelung sum term for this configuration,²⁷ and $V(0)$ is the unperturbed value. The temperature effect is therefore given approximately by

$$\Delta V \cong \left(a_0 \frac{\partial V}{\partial a_0} \right) \left(\frac{\Delta a_0}{a_0} \right) + \left(\epsilon_0 \frac{\partial V}{\partial \epsilon_0} \right) \left(\frac{1}{\epsilon_0} \frac{\partial \epsilon_0}{\partial T} \right) \Delta T \quad (2a)$$

$$\cong +6 \text{ meV} + 170 \text{ meV}, \quad (2b)$$

using the appropriate parameters ($\epsilon_0^{-1} d\epsilon_0/dT \cong 8 \times 10^{-5} \text{ K}^{-1}$ for Si).²⁸ Thus, the change in potential due to the change in effective charge at the bonding and atomic sites can provide a sufficiently large contribution of the correct sign at the Si core to explain the observed temperature shift. We summarize all values in Table I. Although the sum of all one-electron contributions, -245 meV, agrees well with the experimental value, this quantitative agreement should not be taken seriously, because the model presumes an extremely simple spatial charge distribution and does not include the variation of screening with distance.²⁹

V. DISCUSSION

For GaP,⁸ data show that the Ga-3*d* core level contribution to the total temperature dependence of the Ga-3*d* core-conduction-band threshold was negligibly small. For Si, the corresponding data can be explained only on the basis of a relatively *large* shift of the Si-2*p* core level with temperature. We believe that the different behavior results from the different sizes of the core states, the Si-2*p* electrons being significantly more localized than the Ga-3*d* electrons. The radii of these states can be estimated from their binding energies of ~20 eV and ~100 eV and the approximate +5*e* core charge seen by a single core electron, using the screened hydrogenic expressions $E_B = 5 \times 13.6 \text{ eV} / \epsilon^2$ and $r = a_B \epsilon$. Eliminating the dielectric function between the two expressions leads to $r_{2p} \cong 0.8 a_B$ and $r_{3d} \cong 1.8 a_B$ for Si 2*p* and Ga 3*d*, respectively. For comparison, the midpoint of the bond (in either material) is located at approximately $4.5 a_B$. Thus the assumption of a well-localized core-charge distribution, necessary for the validity of the bond-charge calculation, is more realistic for Si 2*p* than for Ga 3*d*. We mention that the larger size of the Ga-3*d* charge distribution influences a number of other phenomena as well, such as the evaluation of effective numbers of electrons n_{eff} by the plasma sum rule. Below the core-level threshold n_{eff} reaches a limiting value of about 4 at the plasma frequency for Si, but continues to rise smoothly with increasing energy through the plasma frequency for GaP.³⁰ The partial hybridization of the Ga-3*d* levels into the valence band that gives rise to the anomalously large number of effective electrons in GaP may also be partly responsible for the different temperature response of the Ga-3*d* core energies.

We comment finally on the implications of these core-level data on the one-electron¹⁻⁵ and lattice-mode^{6,7} models of the temperature dependences of absorption thresholds. For fundamental absorption thresholds between bonding-valence and antibonding conduction-band states, which involve a *difference* between the temperature dependences of the individual states, the models give essentially identical results. But the models predict quite different temperature behavior for the *individual* band edges, although this appears not to have been appreciated. Because core-level spectroscopy can measure in principle the temperature dependence of the conduction-band edge independently from that of the bonding valence-band edge, it provides a possible experimental means of distinguishing between the two models.

Specifically, the one-electron approach, wherein

the one-electron states are perturbed by phonons, predicts that approximately $\frac{1}{3}$ of the temperature dependence of fundamental absorption edges is due to the decrease of the conduction-band energy and $\frac{2}{3}$ to the increase of the valence-band energy with increasing temperature.^{4,5} In the lattice-mode model, the individual contributions can also be calculated. For Si, a hole created at the top of the valence band destroys about 0.9*e* of bond charge (six bonds) while the electron in the conduction-band minimum replaces about 0.05*e* of this.^{7,31} The softening of lattice modes by the net 0.85*e* reduction of the total bond charge produces a decrease of the absorption threshold with increasing temperature. Because the addition of a conduction electron slightly stiffens the lattice, the electronic part alone must cause the conduction-band edge to move to slightly higher energy with increasing temperature. The observed net decrease in the forbidden gap with increasing temperature results from a significantly faster increase of energy of the upper valence levels with increasing temperature. The behavior of the conduction-band edge is thus qualitatively different in the one-electron and lattice-mode models. Unfortunately, it is not yet possible to characterize sufficiently accurately the temperature behavior of core levels to differentiate between the two models on the basis of temperature shifts of the conduction-band edge alone.

Nevertheless, it is possible to show that the lattice-mode model fails quite badly in explaining the Si-2*p* core data obtained here. If one supposes that the contribution of the conduction electron toward the stiffening of the lattice is about the same regardless of whether a core level or an upper valence-band level is the initial state, then the anomalously strong temperature dependence of the core threshold must come from a substantial softening of the lattice (reduction in bond charge) that follows the creation of a core hole. This postulated lattice softening should not result from a gross local distortion of the lattice, because this would imply strong phonon coupling whereas in fact the threshold shows remarkably little broadening. The remaining possibility is the reduction in bond charge resulting from screening the core hole. This can be estimated immediately to be of the order of 2*e* (12 bonds) because the core threshold is observed to vary twice as fast with temperature as the indirect threshold. But this is not possible, because even if the core hole were screened entirely by bond charge, it would not require more charge for screening than that of the hole itself. We conclude that the lattice-mode model fails to describe the temperature dependence of the Si-2*p* conduction-band edge in Si.

VI. CONCLUSION

Our high-resolution reflectance data taken at several different temperatures show that the temperature shifts of the threshold energies of the Si $L_{2,3}$ transitions are surprisingly large, about twice that of the fundamental indirect threshold and in fact exceeding the temperature coefficients⁵ of the direct gaps in most III-V semiconductors. The large values cannot be explained on the basis of conduction-band states alone. A contribution from the core-level states is required as well, which presumably arises from the change in electrostatic potential at the $2p$ core as a result of a temperature-induced redistribution of valence charge. A simple model calculation suggests this, although these calculations have only qualitative validity because the detailed nature of the large final-state excitation¹⁶ is not clear. The apparent absence of core-level effects in the Ga- $3d$ core transition of GaP appears to be due to the much larger volume occupied by the Ga- $3d$ core hole, which provides greater spatial averaging of the potential change resulting from charge redistribution.

The thermorefectance data show in addition that the threshold shift accounts for nearly all of the effect of temperature on these transitions: thermal broadening effects are essentially nonexistent. The TR results also show that the temperature shift of the $2p_{1/2}$ component exceeds that of the $2p_{3/2}$ component. Similar behavior has been observed in sp^3 valence-conduction-band transitions in several zinc-blende-structure semiconductors.²¹ The TR signals were large, but owing to the ne-

cessity of modulating at very low frequencies (0.5 Hz), we were unable to take full advantage of the technique. With the current state of the art, we found that numerically differentiated high-resolution reflectance data, which were less affected by low-frequency noise, were superior; however, all modulation techniques should have much to offer in this spectral range.

We note finally that we have assumed throughout that the temperature dependence of the "binding energy" (difference between the ground state and ionization state) of the conduction-electron- $L_{2,3}$ -core-hole excitation is negligible. Since the temperature dependences of the indirect gap and the $L_{2,3}$ exciton threshold are now both known, this assumption can be checked easily by measuring the temperature dependence of the energy separation between the core electrons and the top of the valence band by photoemission or energy-loss measurements. If this assumption is correct, we should expect to find an approximately 125 meV decrease in this separation from 150 to 600 K. An energy difference of this magnitude should be easily measurable by current techniques.

ACKNOWLEDGMENTS

It is a pleasure to acknowledge the cooperation of H. Winick and the staff of the Stanford Synchrotron Radiation Project where the measurements were performed. The Stanford Synchrotron Research Project is supported in part by the NSF Grant No. DMR 73-07692 in cooperation with the Stanford Linear Accelerator Center and the U. S. ERDA.

[†]Work at the Max-Planck-Institut supported in part by an Alexander von Humboldt Senior Scientist Award.

*Permanent address.

¹S. C. Yu and H. Brooks (unpublished); J. P. Waller, R. R. L. Zucca, M. L. Cohen, and Y. R. Shen, *Phys. Rev. Lett.* **24**, 102 (1970); D. Auvergne, J. Camassel, H. Mathieu, and M. Cardona, *Phys. Rev. B* **9**, 5168 (1974).

²P. Y. Yu and M. Cardona, *Phys. Rev. B* **2**, 3193 (1970).

³H. Y. Fan, *Phys. Rev.* **82**, 900 (1951); Yu. I. Ravich, *Fiz. Tverd. Tela* **7**, 1821 (1965) [*Sov. Phys.-Solid State* **7**, 1466 (1965)].

⁴K. Baumann, *Phys. Status Solidi B* **63**, K71 (1974).

⁵J. Camassel and D. Auvergne, *Phys. Rev. B* **12**, 3258 (1975).

⁶H. Brooks, *Adv. Electron.* **7**, 85 (1955); V. Heine and C. H. Henry, *Phys. Rev. B* **11**, 3795 (1975).

⁷V. Heine and J. A. Van Vechten, *Phys. Rev. B* **13**, 1622 (1976).

⁸D. E. Aspnes, C. G. Olson, and D. W. Lynch, *Phys. Rev. Lett.* **36**, 1563 (1976).

⁹H. Fujita, Y. Iguchi, Y. Okada, and T. Sasaki, *J. Phys. Soc. Jpn.* **33**, 1494 (1972).

¹⁰H. Fujita and Y. Iguchi, *Jpn. J. Appl. Phys.* **14**, 220 (1975).

¹¹R. Z. Bachrach, F. C. Brown, and M. Skibowski, *Bull. Am. Phys. Soc.* **20**, 488 (1975); F. C. Brown, R. Z. Bachrach, and M. Skibowski, *Phys. Rev. B* **15**, 4781 (1977).

¹²F. C. Brown and O. P. Rustgi, *Phys. Rev. Lett.* **28**, 497 (1972).

¹³F. C. Brown, in *Solid State Physics*, edited by F. Seitz, D. Turnbull, and H. Ehrenreich (Academic, New York, 1974), Vol. 29, p. 1. See particularly, Figs. 25 and 26 and the accompanying discussion.

¹⁴D. E. Aspnes, C. G. Olson, and D. W. Lynch, *J. Appl. Phys.* **47**, 602 (1976).

¹⁵R. Z. Bachrach, in *Proceedings of the International Workshop on the Development of Synchrotron Radiation Facilities, Quebec City* (Centre for Interdisciplinary Studies in Chemical Physics, University of Western Ontario, London, 1976), pp. 9-49.

- ¹⁶R. S. Bauer, R. Z. Bachrach, J. C. McMnamin, and D. E. Aspnes, *Nuovo Cimento B* **39**, 409 (1977).
- ¹⁷C. D. Thurmond, *J. Electrochem. Soc.* **122**, 1133 (1975).
- ¹⁸R. K. Kirby, T. A. Hahn, and B. D. Rothrock, in *American Institute of Physics Handbook*, 3rd ed., edited by D. E. Gray (McGraw-Hill, New York, 1972), pp. 4-129.
- ¹⁹G. G. Macfarlane, T. P. McLean, J. E. Quarrington, and V. Roberts, *J. Phys. Chem. Solids* **8**, 388 (1959).
- ²⁰W. Bludau, A. Onton, and W. Heinke, *J. Appl. Phys.* **45**, 1846 (1974).
- ²¹E. Matatagui, A. G. Thompson, and M. Cardona, *Phys. Rev.* **176**, 950 (1968).
- ²²J. R. Chelikowsky and M. L. Cohen, *Phys. Rev. B* **10**, 5095 (1974).
- ²³W. G. Spitzer and H. Y. Fan, *Phys. Rev.* **108**, 268 (1957); M. Balkanski, A. Aziza, and E. Amzallag, *Phys. Status Solid.* **31**, 323 (1969); R. A. Forman, W. R. Thurber, and D. E. Aspnes, *Solid State Commun.* **14**, 1007 (1974); R. Hulthén and N. G. Nilsson, *ibid.* **18**, 1341 (1976).
- ²⁴M. Cardona, in *Atomic Structure and Properties of Solids*, edited by E. Burstein (Academic, New York, 1972), p. 514.
- ²⁵M. L. Cohen and V. Heine, in Ref. 13, 1971, Vol. 24, p. 37.
- ²⁶J. C. Phillips, *Phys. Rev.* **166**, 832 (1968); **168**, 905, 912, 917 (1968); *Phys. Lett. A* **37**, 434 (1971).
- ²⁷R. M. Martin, *Phys. Rev.* **186**, 871 (1969).
- ²⁸M. Cardona, W. Paul, and H. Brooks, *J. Phys. Chem. Solids* **8**, 204 (1959).
- ²⁹J. S.-Y. Wang and C. Kittel, *Phys. Rev. B* **7**, 713 (1973).
- ³⁰H. R. Philipp and H. Ehrenreich, in *Semiconductors and Semimetals*, Vol. 3, edited by R. K. Willardson and A. C. Beer (Academic, New York, 1966), p. 93.
- ³¹C. V. de Alvarez and M. L. Cohen, *Solid State Commun.* **14**, 317 (1974).